

# Increasing the possibility of using thermoanemometric type heat exchangers in the control of man-made objects

Rayimjonova O.S., Nurdinova R.A., Dalibekov L.R, Ergashev Sh.

Teachers of the Fergana branch of the Tashkent University of Information Technologies named after Muhammad al-Kharazmiy, the city of Fergana, the country of Uzbekistan

**ABSTRACT:** This work analyzes the research of sensors for monitoring the parameters of technogenic objects. The results of the experiment of creating sensors for measuring the gas velocity in control and monitoring systems are presented. The advantages of thermal converters of thermoanemometric type are determined.

## LINTRODUCTION

The application of the latest achievements of science and technology in the developed countries, including the Republic, in the fields of national economy, industry and production impose the task of researchers to develop and create measures to prevent accidents that may occur as a result of these applications.

Heat and wind energy, construction of high-rise buildings, metallurgy, construction of oil and gas complexes require special attention to monitoring the parameters of the external environment for their uninterrupted operation. This requires obtaining accurate information about the properties of controlled technical objects, various technological parameters, as well as research on the development of systems for monitoring and control of the state of technical units operating in complex climatic and aggressive conditions.

One of the solutions to the problems of metrological supply at the level of modern requirements is to improve its functionality, performance reliability, high accuracy, speed to improve the variables of gas flow parameters in control and monitoring systems.

## II. PROBLEM STATEMENT

A generalized functional diagram of a hybrid converter designed to control the velocity and direction of gas flow is shown in Fig. 1.

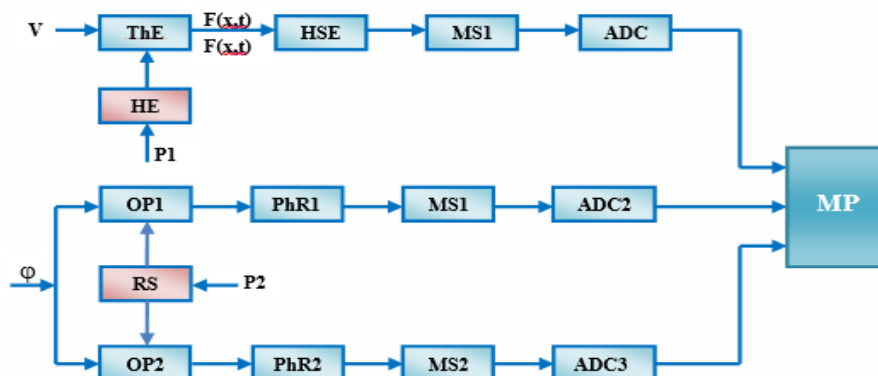


**Fig. 1.** Generalized functional scheme of a hybrid converter designed to control the speed and direction of gas flow:  $V$  - gas flow rate,  $m/s$ ;  $\varphi$  - the angle of rotation of the flow direction; HE - heating element; RS - radiation source; ThE - thermal element; HSE - heat-sensitive element; OS1, OS2 - optical screens; P1, P2 - power supply; MS1, MS2, MS3 -

measurement schemes; PhR1, PhR2- photoresistors; ADC1, ADC2, ADC3 - analog-to-digital converters; MP – microprocessor

As shown above [1], the design of a hybrid converter for open gas flow includes a heat exchanger to measure the horizontal wind speed and determine the temperature [2], which is made in the form of a copper tube mounted vertically on the surface of the housing.

To obtain a mathematical model of the speed sensor, the physical models of the speed sensors [3] with the thermocouple and heating element correspond to the three models a.

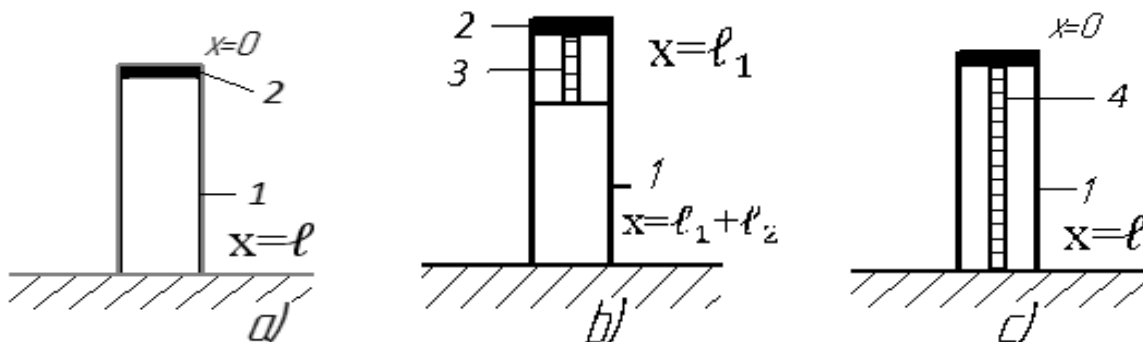


**Fig. 2.** Physical models of wind (gas flow) speed sensors. 1-heat conductor; 2-integrated heating element; 3-heating element distributed in a limited area of the heat conductor; 4-heating element distributed along the entire length of the heat conductor

We consider a method of constructing mathematical models for the options described in Fig. 2, which is widely used to measure both velocity and airflow temperature T. In this case, the combined thermoelectric elements and distributed heat-sensitive elements can be used as shown in Fig. 2.

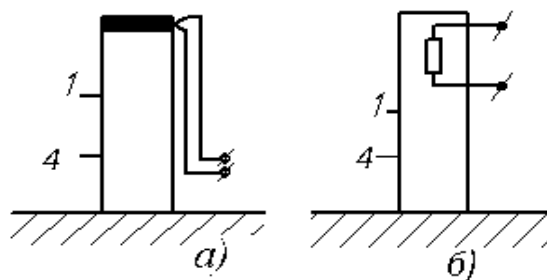


**Fig. 3.** Scheme of placement of integrated heating elements and distributed heat-sensitive elements in the form of thermoelectric thermometers and semiconductor resistance thermometers.

In solving mathematical models of velocity heat sensors, it is expedient to look at their heating systems as quadrupoles, in which temperature T and heat flux F are taken as input and output magnitudes [4, 5, 6, 7, 8].

A convenient form of writing a mathematical model for the heating system in Fig. 2A, is to write the temperature  $T_{1(0,p)}$  and heat flux  $\Phi_{1(0,p)}$  at its beginning ( $x = 0$ ), the temperature  $T_{2(l,p)}$  and heat flux  $\Phi_{2(l,p)}$  (and their images) for the heat conductor  $1 \ x = l$  [9]:

$$\begin{aligned} T_{1(0,p)} &= AT_{2(l,p)} + B\Phi_{2(l,p)}; \\ \Phi_{1(0,p)} &= CT_{2(l,p)} + D\Phi_{2(l,p)}, \end{aligned} \tag{1}$$

A, B, C, D are the matrix-shaped parameters of the four poles of heat, and these equations take the following form:

$$\begin{vmatrix} T_{1(0,p)} \\ \Phi_{1(0,p)} \end{vmatrix} = \begin{vmatrix} A & B \\ C & D \end{vmatrix} \begin{vmatrix} T_{2(l,p)} \\ \Phi_{2(l,p)} \end{vmatrix}. \tag{2}$$

To determine the temperature and heat flux, we change these equations to the following:

$$\begin{vmatrix} T_{(x,p)} \\ \Phi_{(x,p)} \end{vmatrix} = \begin{vmatrix} A_{(x,p)} & B_{(x,p)} \\ C_{(x,p)} & D_{(x,p)} \end{vmatrix} \begin{vmatrix} T_{1(0,p)} \\ \Phi_{1(0,p)} \end{vmatrix}, \tag{3}$$

Using expression (2.1), we can determine the parameters of the four poles of heat from the following expressions:

$$A_{(x,p)} = ch[\gamma(p), x], \tag{4}$$

$$B_{(x,p)} = -z(p)sh[\gamma(p), x], \tag{5}$$

$$C_{(x,p)} = -\frac{1}{z(p)}sh[\gamma(p), x], \tag{6}$$

$$D_{(x,p)} = ch[\gamma(p), x], \tag{7}$$

(4), (5), (6) and (7) and are defined by the following formulas:

$$\gamma(p) = \sqrt{r(cp + g)}, \tag{8}$$

$$z(p) = \sqrt{\frac{r}{(cp + g)}}, \tag{9}$$

$g = \alpha \pi d$  is the specific thermal conductivity corrected per unit length of the heat conductor;  $-\alpha$  coefficient of heat separation from the heat conductor  $\pi = 3,14$ ;  $d$  is the diameter of the heat conductor;  $r = \frac{1}{\lambda F}$  specific heat resistance per unit length of heat conductor;  $\lambda$  thermal conductivity of heat-conducting material;  $S = \frac{\pi d^2}{4}$  the cutting surface of the heat conductor;  $C = \rho C_p F$  specific heat capacity per unit length of heat conductor;  $\rho$  - density of heat-conducting material;  $C_p$  - specific heat capacity of heat conductor material;  $p$  - Laplace operator.

For the sake of simplification, we assume that the parameters  $r$ ,  $c$ , and  $g$  are uniformly distributed, i.e., and, and that the equation of the matrices (3) has the following form:

$$\begin{vmatrix} T_{(x,p)} \\ \Phi_{(x,p)} \end{vmatrix} = \begin{vmatrix} ch[\gamma(p)x] & -z(p)sh[\gamma(p)x] \\ -\frac{1}{z(p)}sh[\gamma(p)x] & ch[\gamma(p)x] \end{vmatrix} \begin{vmatrix} \theta_{1(0,p)} \\ \Phi_{1(0,p)} \end{vmatrix}, \tag{10}$$

From Equation (10) we find:

$$\begin{aligned} T_{(x,p)} &= T_{1(x,p)}ch[\gamma(p)x] - \Phi_{1(0,p)}z(p)sh[\gamma(p)x], \\ \Phi_{(x,p)} &= -\frac{T_{1(x,p)}}{z(p)}sh[\gamma(p)x] + \Phi_{1(0,p)}ch[\gamma(p)x]. \end{aligned} \tag{11}$$

For the heating circuit in question:

$$T_{1(0,p)} = z(p)\Phi_{1(0,p)}, \tag{12}$$

and the extinction of the heatwave is high, in which case the thermal resistance  $z(p)$  of the heat chain is equal to:

$$z(p) = z_{kup}(p) = \sqrt{\frac{r}{(cp + g)}}. \tag{13}$$

In this case, to determine the temperature, we use (11, 12, 13) to create the following expression:

$$T_{(x,p)} = \Phi_{1(0,p)}z(p) \{ch[\gamma(p)x] - sh[\gamma(p)x]\} = \Phi_{1(0,p)}z(p)e^{-\gamma(p)x} \tag{14}$$

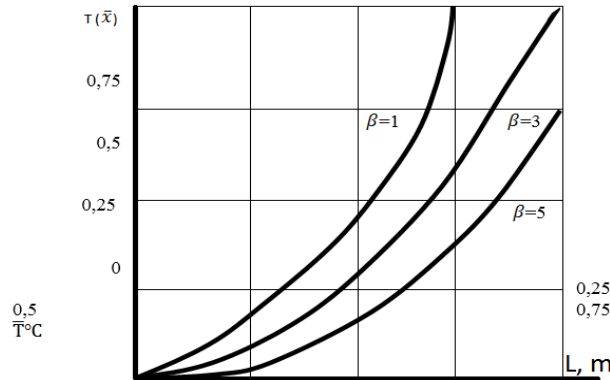


Fig. 4. Graphs of temperature  $T(x)$  distribution along the length of a heat conductor

Fig. 3 shows  $d = 4 \cdot 10^{-3}$  m graphs of  $T(x)$  temperature distribution along the length of a heat conductor from an m diameter copper pipe.

$\bar{T}(x) = T(x)/T(0)$  we determine the relative values  $\bar{x} = x/x_M$  by entering  $\beta = x_M$  the coordinates, and we get the equation

$$\bar{T}(\bar{x}) = \exp(-\beta \bar{x}) \tag{15}$$

The expression for the stationary operating mode of the speed heat sensor has the following appearance

$$T(x) = \phi_1(0)ze = \phi_1(0)\sqrt{\frac{r}{g}}g^{-\sqrt{gr}x} \text{ or } \bar{T}(\bar{x}) = \exp(-\beta \bar{x}). \tag{16}$$

For the variant in Fig. 2, 6, the heat conductor consists of two spheres: a sphere with a distributed heating element 3 and a heat conductor 1 (without a heating element). Based on Equation (10), the following equation can be written for field 3:

$$T_1(x) = T_1(0)ch\gamma x + \frac{q}{g}(1 - ch\gamma x) = \left[ \bar{T}_1(0) - \frac{q}{g} \right] ch\gamma x + \frac{q}{g},$$

$$V_1 = 1,0 \frac{c}{M}, V_2 = 0,7 \frac{c}{M}, V_3 = 0,4 \frac{c}{M}. \tag{17}$$

The equation for the field looks like this:

$$T_2(x) = T_2(l)ch\gamma_2 x + z_2\Phi_2(l_2)ch\gamma_2 x = T_2(l_1)e^{-\gamma(p)x}, \tag{18}$$

$T(x)$  The temperature distribution equation distributed over the entire area of the heat conductor 1 has the following form:

$$T(x) = T(0)ch\gamma x - \Phi(0)zch\gamma x + q(ch\gamma x)/g, \tag{19}$$

Fig. 4 shows the  $\beta$  curves of the variation of  $T(x)$  different values.

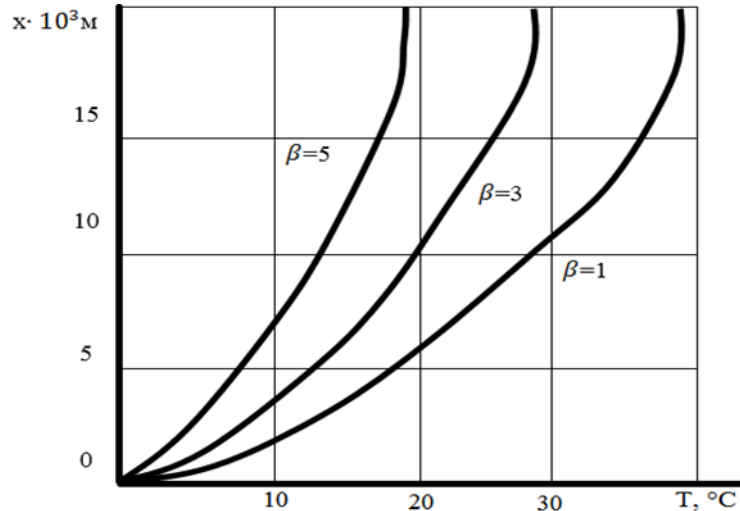


Fig. 5. Distribution graphs of  $T(x)$  different values  $\beta$

As shown above, heat conductors are fitted with heat-sensitive elements that allow information on both the velocity and temperature of the flow to be obtained.

### III. DESCRIPTION OF THE METHOD FOR SOLVING THE RESEARCH PROBLEM

An experimental study of the design of heat exchangers was carried out to obtain preliminary data in the design of heat exchangers and to establish that the mathematical models correspond to real descriptions. Experimental studies are the study of the dependence of the electrical resistance of semiconductor cylindrical thermocouples of type MMT-1 on different velocities  $v$  of airflow, in which the data are processed in the form of dependence of the average temperature  $\bar{T}_{av}$  on airflow velocities  $v$  and their calculated values based on mathematical models. comparison is performed.

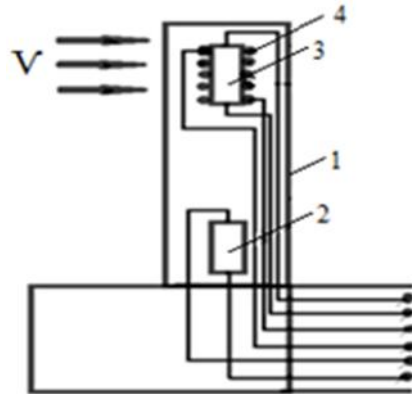
The scheme of the experimental study of samples of transducers was carried out on the device shown in Fig. 6



Fig. 6. Scheme of the experimental device for the study of thermoanemometric type heat exchangers: 1 – thermoanemometric type heat exchanger; 2-RS-ZA type rotameter; 3 GSB 400 gas meter; 4 consumption motor (pump)

Fig. 7 shows the experimental design of a thermoanemometric transducer based on two MMT-1 types of semiconductor resistors  $d_T = 2 \cdot 10^{-3}$  m diameter and  $l_T = 12 \cdot 10^{-3}$  m length),  $d = 8 \cdot 10^{-3}$  m, m diameter glass tube.

The results of the computational and experimental studies are shown in Fig. 8: Graphic 1 corresponds to the dependence of the  $R_T$  resistance of 2 on the velocity  $V$ . This description is taken for  $R_T$  the heating element. Figs. 2, 3, and 4 show that the resistance of the heating element 4 to the resistance of the heating element 4 corresponds to the airflow rate  $V$  flowing through the heating element  $2 - I_{HE} = 0,045$  A ;  $3 - I_{HE} = 0,07$  A ;  $4 - I_{HE} = 0,1$  A corresponds to the dependencies in the currents.



**Fig. 7.** Experimental design of the heat exchanger for airflow parameters: 1-glass tube; Semiconductor thermodynamics of type 2 without heating element MMT-1 (Ohm, kOhm, kOhm, at  $T = 20\text{ }^{\circ}\text{C}$ ); 3-conductor semiconductor thermocouple, 4-manganese wire heating element

The computational and experimental data (the lines represent the computational data and the dots represent the experimental data) show that they are well-matched, which confirms the correctness of the method of constructing mathematical models and the method of calculation. Fig. 8 shows  $I_{HE} = 0,07\text{ A}$  graphs of the differences between the mean temperature  $\bar{T}(x)$  and airflow  $T_0$  temperature for current resistance in the current.

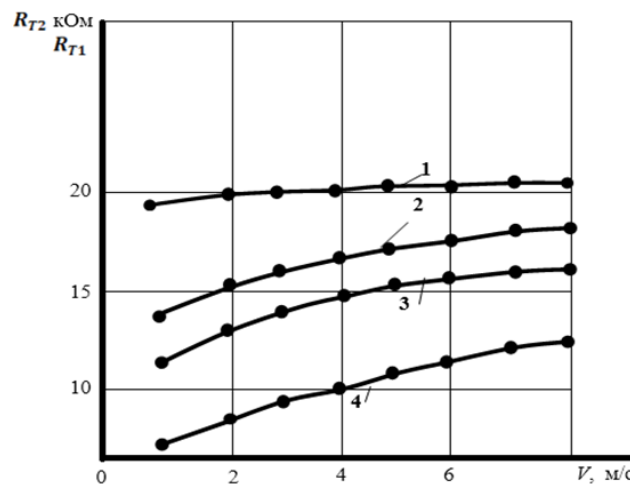


**Fig. 8.** Graphs of the dependence of the airflow velocity V on the thermal resistances 2 and 3 in the experimental design (Fig. 7)

1, 2 - experimental graphs obtained without a heating element; 3, 4 - Experimental graphs obtained on the heating element

In calculating the dependencies  $R_T = f(v)$  (pic 2.7) and  $\Delta T = \bar{T}(x) - T_0$  (pic 2.9), it was taken into account that in such semiconductor with heating element resistors, the heat released from heating element cannot be fully absorbed by the resistor and part of the heat is lost (thermal contact with heating element is ideal). not with radiation and heat loss on the connecting wires).

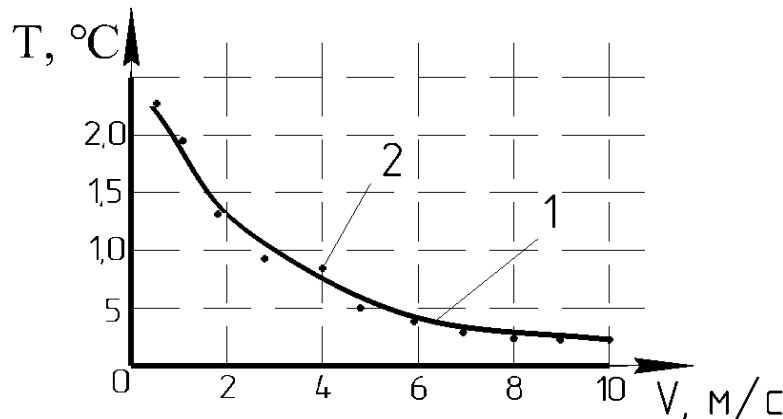


Fig. 9. Graph of temperature difference  $\Delta T$  as a function of airflow velocity  $V$ : 1-calculation data (lines); 2 - experimental data (points)

#### IV. CONCLUSION

Therefore, as in the study, we introduced the coefficient of thermal contact, the value of  $K_{TC}$  0,5 – 0,97 which was calculated by comparing the heating resistance of heating degree with and without heating element, and determined based on experimental data [64]. In our study,  $K_{TC} = 0.49$ , and  $K_{TC}$  based on the heat losses, it was possible to determine the good compatibility of the calculation and experimental data (the difference does not exceed 8-10%).

$$\Delta T = \bar{T}(x) - tT_0, \text{ } ^\circ\text{C} . \quad (19)$$

Analysis of the results of experimental and theoretical studies shows that the smallest sensitivity of heating element you have a place in thermoanemometric type heat exchangers where it is necessary to increase the current flowing through the thermocouple in the bridge measurement circuit to increase the sensitivity of thermoanemometric type heat exchangers, but this practice leads to a decrease. Thermoanemometric type heat exchangers with thermal elements have the best description and therefore they are selected for further research and development.

#### REFERENCES

1. Grechishnikov V.M., Konyukhov N.E. Optoelectronic digital displacement sensors with built-in fibre-optic communication lines, Moscow, Energoatomizdat Publ., 1992, 152 p. (In Russian).
2. Azimov R.K., Shipulin Yu.G., Rayimjanova O.S. Patent Republic of Uzbekistan, no IAP 04754, dated 21.02.2013. (In Russian).
3. Azimov R.K., Azimov A. Thermal transformers speed and direction of gas flows and liquids, Moscow, Energoatomizdat Publ., 1990, 60 p. (In Russian).
4. Eisenberg Yu.B., Buxman G.B., Korobko A.A., Pyatigorskiy V.M. Hollow long light conductors at the present stage, lighting engineering, 2003, no.3, pp.14-23. (In Russian).
5. Azimov R.K., Shipulin Yu.G., Siddikov I.X. Analysis of static characteristics of optoelectronic primary transducers based on extended light guides, Materials of the seminar "Application of optical-electronic devices and fiber optics in the national economy", 1989, pp.141-149. (In Russian).
6. Azimov R.K., Shipulin Yu.G. Optoelectronic converters of large movements based on hollow waveguides, Moscow, Energoatomizdat Publ., 1987, 105 p. (In Russian).
7. Azimov R.K., Shipulin Yu.G. Khodzhaev S.S., Siddikov I.Kh. Graph models of optoelectronic primary converters, Reports of the Academy of Sciences of the Republic of Uzbekistan, 1997, no 6, pp.12-15. (In Russian).
8. Azimov R.K., Shipulin Yu.G. Discrete optoelectronic converters based on hollow waveguides for monitoring systems and level and flow, Collection of scientific reports of the II th International Scientific, Theoretical and Practical Conference "Problems and Prospects of Automation of Production and Management", 1999, pp.108-116. (In Russian).
9. Azimov R.K., Shipulin Yu.G. Mathematical models of optoelectronic converters based on hollow waveguides, Collection of scientific works "Photovoltaic and fibre-optic converters for control and computer systems" Kuibyshev Aviation Institute, Samara, 1986, pp.104-113. (In Russian).